

[Ca²⁺]_i oscillations in human sperm are triggered in the flagellum by membrane potential- sensitive activity of CatSper

Elis Torrezan-Nitao
Sean G. Brown
Esperanza Mata-Martínez
Claudia L. Treviño
Christopher Barratt
Stephen Publicover

This is a pre-copyedited, author-produced version of an article accepted for publication in Human Reproduction following peer review. The version of record

Torrezan-Nitao, E., Brown, S.G., Mata-Martínez, E., Treviño, C.L., Barratt, C. & Publicover, S. (2020) '[Ca²⁺]_i oscillations in human sperm are triggered in the flagellum by membrane potential- sensitive activity of CatSper'. *Human Reproduction*.

is available online at:

<https://doi.org/10.1093/humrep/deaa302>

[Ca²⁺]_i oscillations in human sperm are triggered in the flagellum by membrane potential-sensitive activity of CatSper

¹Elis Torrezan-Nitao, ²Sean G. Brown, ³Esperanza Mata-Martínez, ³Claudia L. Treviño, ⁴Christopher Barratt, and ¹Stephen Publicover

¹School of Biosciences, University of Birmingham, Birmingham

²School of Applied Sciences, Abertay University, Dundee DD11HG, UK

³Departamento de Genética del Desarrollo y Fisiología Molecular, Instituto de Biotecnología, Universidad Nacional Autónoma de México, Cuernavaca, Morelos 62210, México

⁴Systems Medicine, Ninewells Hospital and Medical School, University of Dundee, Dundee, DD19SY, UK

Running title: Vm and CatSper trigger sperm Ca²⁺ oscillations

Key words: sperm, Ca²⁺ oscillation, CatSper, membrane potential, RU1968

22 Abstract

23 **Study question:** How are progesterone (P4)-induced repetitive intracellular Ca^{2+} concentration
24 ($[\text{Ca}^{2+}]_i$) signals (oscillations) in human sperm generated?

25 **Summary answer:** P4-induced $[\text{Ca}^{2+}]_i$ oscillations are generated in the flagellum by membrane-
26 potential (V_m)-dependent Ca^{2+} -influx through CatSper channels, which then induce secondary Ca^{2+}
27 mobilisation at the sperm head/neck region.

28 **What is known already:** A subset of human sperm display $[\text{Ca}^{2+}]_i$ oscillations that regulate flagellar
29 beating and acrosome reaction. Though pharmacological manipulations indicate involvement of
30 stored Ca^{2+} in these oscillations, influx of extracellular Ca^{2+} is also required.

31 **Study design, size, duration:** This was a laboratory study, that used >20 sperm donors and involved
32 more than 100 separate experiments and analysis of more than 1,000 individual cells over a period of
33 2 years.

34 **Participants/materials, setting, methods:** Semen donors and patients were recruited in accordance
35 with local ethics approval from Birmingham University and Tayside ethics committees. $[\text{Ca}^{2+}]_i$
36 responses and V_m of individual cells were examined by fluorescence imaging and whole-cell current
37 clamp.

38 **Main results and the role of chance:** P4-induced $[\text{Ca}^{2+}]_i$ oscillations originated in the flagellum,
39 spreading to the neck and head (latency of 1-2 s). K^+ -ionophore valinomycin (1 μM) was used to
40 investigate the role of membrane potential (V_m). Direct assessment by whole-cell current-clamp
41 confirmed that V_m in valinomycin-exposed cells was determined primarily by K^+ equilibrium
42 potential (E_K) and was rapidly 'reset' upon manipulation of $[\text{K}^+]_o$. Pretreatment of sperm with
43 valinomycin ($[\text{K}^+]_o=5.4 \text{ mM}$) had no effect on the P4-induced $[\text{Ca}^{2+}]$ transient ($P=0.95$; 8
44 experiments), but application of valinomycin to P4-pretreated sperm suppressed activity in 82% of
45 oscillating cells ($n=257$; $P=5 \times 10^{-55}$ compared to control) and significantly reduced both amplitude
46 and frequency of persisting oscillations ($p=0.0001$). Upon valinomycin washout oscillations re-started
47 in most cells. When valinomycin was applied in saline with elevated $[\text{K}^+]$ the inhibitory effect of

valinomycin was reduced and was dependent on E_K ($P=10^{-25}$). Amplitude and frequency of $[Ca^{2+}]_i$ oscillations that persisted in the presence of valinomycin showed similar sensitivity to E_K ($P<0.01$). The CatSper inhibitor RU1968 (4.8 and 11 μM) caused immediate and reversible arrest of activity in 36% and 96% of oscillating cells respectively ($P<10^{-10}$). 300 μM quinidine which blocks the sperm K^+ current (K_{sper}) completely inhibited $[Ca^{2+}]_i$ oscillations.

Large scale data: n/a

Limitations, reasons for caution: This was an in-vitro study and caution must be taken when extrapolating these results to in vivo regulation of sperm.

Wider implications of the findings: $[Ca^{2+}]_i$ oscillations in human sperm are functionally important and their absence is associated with failed fertilisation at IVF. The data reported here provide new understanding of the mechanisms that underlie the generation (or failure) and regulation of these oscillations.

Study funding/competing interest(s): ET was in receipt of a postgraduate scholarship from the CAPES Foundation (Ministry of Education, Brazil). The authors have no conflicts of interest.

Introduction

Ca²⁺-signalling plays an essential role in the regulation of sperm cell function. Key activities, including motility, acrosome reaction and capacitation (acquisition of fertilising ability) are regulated through intracellular calcium concentration ([Ca²⁺]_i) and can be modified by artificial manipulation of Ca²⁺-signalling processes (Darszon, et al., 2011, Publicover, et al., 2007, Suarez, 2008). In most animal phyla the primary plasma membrane Ca²⁺ channel of sperm is CatSper (Cai and Clapham, 2008, Ren, et al., 2001), which can be activated upon encountering a stimulus, generating an immediate increase in cytoplasmic [Ca²⁺] and a consequent change in the activity of the cell. For instance, in sea urchin sperm, activation of CatSper induced by binding of chemoattractant molecules to their receptors (Seifert, et al., 2015) induces a transient elevation of [Ca²⁺]_i that causes the sperm to re-orientate its path up the chemoattractant gradient (Guerrero, et al., 2010, Kaupp, et al., 2008). Similarly, in human sperm activation of CatSper channels by progesterone (P4) results in a [Ca²⁺]_i transient which induces a brief, but marked, modification of flagellar beating (Bedu-Addo, et al., 2007, Schiffer, et al., 2014, Smith, et al., 2013).

As well as phasic Ca²⁺ signals that are induced upon presentation of a stimulus, human sperm generate repetitive [Ca²⁺]_i spikes or oscillations, either during prolonged exposure to a stimulus or even ‘spontaneously’, in the absence of any applied stimulus (Harper, et al., 2004, Mata-Martinez, et al., 2018). The functional significance of these signals is not clear. Initial observations on loosely immobilised cells exposed to a prolonged P4 stimulus showed that each [Ca²⁺]_i spike or oscillation peak was associated with a temporary increase in the amplitude of flagellar excursion (Harper, et al., 2004), suggesting that these signals may be involved in regulation of flagellar beat mode. More recently it has been shown that occurrence of acrosome reaction is suppressed in cells displaying spontaneous [Ca²⁺]_i oscillations (Sanchez-Cardenas, et al., 2014) and that ability to undergo acrosome reaction can be restored by inhibition of these [Ca²⁺]_i signals (Mata-Martinez et al, 2018). The occurrence of samples that completely failed to generate [Ca²⁺]_i oscillations in response to P4 was significantly higher in men who failed to fertilise at IVF compared to samples from donors and patients who fertilised (Kelly, et al., 2018).

Repetitive $[Ca^{2+}]_i$ activity in somatic cells is typically generated by mobilisation of Ca^{2+} stored in intracellular organelles, such as the endoplasmic reticulum. Upon stimulation the storage organelles are cyclically emptied (by activation of Ca^{2+} channels) and refilled (by activity of Ca^{2+} -ATPases) resulting in an oscillatory Ca^{2+} signal (Berridge, et al., 1988, Berridge, et al., 2003). Sperm cells appear to possess at least two Ca^{2+} storage organelles which have Ca^{2+} channels and Ca^{2+} -ATPases similar to those in somatic cells (Correia, et al., 2015, Costello, et al., 2009) and pharmacological studies indicate that these stores are involved in the generation of oscillatory Ca^{2+} signals in human sperm (Harper, et al., 2004, Mata-Martinez, et al., 2018). However, in both excitable and non-excitable cells, oscillation of $[Ca^{2+}]_i$ can also occur due to interaction between voltage-sensitive Ca^{2+} channels and Ca^{2+} sensitive K^+ channels, resulting in cyclic changes in membrane potential (V_m) and consequent bursts of Ca^{2+} -influx (e.g. Gorman and Thomas, 1978, Lopez, et al., 1995, Schlegel, et al., 1987). Significantly, though stored Ca^{2+} is implicated in the mechanism underlying Ca^{2+} oscillations in human sperm, extracellular Ca^{2+} is required for their generation and/or persistence (Harper, et al., 2004, Mata-Martinez, et al., 2018) suggesting that regulation of membrane Ca^{2+} permeability is involved in generating or shaping repetitive $[Ca^{2+}]_i$ activity. We have therefore investigated the initiation of $[Ca^{2+}]_i$ oscillations in human sperm and the potential involvement of CatSper and regulation by V_m .

Methods

Materials All chemicals were obtained from Sigma-Aldrich (Poole, UK) except fluo4-AM (acetoxymethylester), which was from Thermo Fisher Scientific, UK. Fluo4-AM was prepared in dimethylsulphoxide (DMSO) containing 20% Pluronic F-127 (Thermo Fisher). P4 and RU1968 were dissolved in DMSO at 10 mM and diluted in sEBBS prior to use. Quinidine was dissolved in DMSO at 100 mM and diluted in sEBBS prior to use. RU1968 was a kind gift of Dr Timo Strücker, Centre of Reproductive Medicine and Andrology, Münster, Germany,

Salines The standard incubation medium used in this study was supplemented Earle's balanced salt solution (sEBSS), containing NaCl (90 mM), KCl (5.4 mM), CaCl₂ (1.8 mM), MgCl₂ (1 mM), glucose (5.5 mM), NaHCO₃ (25 mM), Na pyruvate (2.5 mM), Na lactate (19 mM), MgSO₄ (0.81 mM), HEPES (15 mM) and 0.3% bovine serum albumin (BSA). The pH was adjusted to 7.4 with NaOH and osmolality was then adjusted to 291-294 mOsm as necessary by adding NaCl. Salines with increased [K⁺] were made by isotonic replacement of NaCl with KCl. 'Ca²⁺-free' saline was made by omission of CaCl₂ ([Ca²⁺]_i < 5 µM; Harper, et al., 2004) and in EGTA-buffered saline CaCl₂ was omitted and 2 mM EGTA was added (calculated [Ca²⁺]_i = 2.6 * 10⁻¹⁰ M; Maxchelator (Webmaxc standard); UC, Davis). Intracellular (pipette) solution for current clamp recordings contained NaCl (10 mM), KCl (18 mM), K gluconate (92 mM), MgCl₂ (0.5 mM), CaCl₂ (0.6 mM), EGTA (1 mM), HEPES (10 mM), pH adjusted to 7.4 using KOH, which brought [K⁺]_i to 114 mM and [Ca²⁺]_i to 0.11 µM (Webmaxc standard).

Selection and preparation of spermatozoa Written consent was obtained from donors in accordance with the Human Fertilisation and Embryology Authority (HFEA) Code of Practice (version 8) under local ethical approval (University of Birmingham (ERN 07-009 and ERN-12-0570) and Tayside Committee of Medical Research Ethics (13/ES/0091)). Semen samples were from donors with normal sperm concentration and motility (measured parameters for all samples exceeded the lower reference limits; WHO 2010; table S1). Samples were obtained by masturbation after 2-3 days sexual

abstinence. After liquefaction (30 min), sperm were swum up into sEBSS (60 min), adjusted to a maximum of ≈ 6 million/ml and left to capacitate (36°C , 5.5% CO_2) for 5 hours.

Current Clamp

To monitor membrane V_m directly, electrophysiological recordings were conducted on sperm, bathed in sEBSS, using whole-cell, zero current clamp. Recording pipettes were filled with standard intracellular solution and gigaseals were achieved by carefully manoeuvring the tip of the pipette onto the neck region of the sperm and applying gentle suction. This was followed by another brief suction to achieve the whole-cell configuration. Data were acquired at 5 KHz and low pass filtered at 3 KHz using an Axopatch 200B (Molecular Devices). Data presented are adjusted for liquid junction potential.

Collection and analysis of imaging data. Imaging was carried out essentially as described in (Nash, et al., 2010). Briefly, after adjusting cell concentration to 1.5×10^6 million/ml the cell suspension was divided into aliquots of 200 μL and incubated with fluo4-AM (5 μM) for 30 min (36°C , 5.5% CO_2). Cells were then transferred to a perfusable imaging chamber, the base of which was a coverslip coated with 0.001% poly-D-lysine and incubated for an additional 5 minutes to allow cells to settle. The chamber was installed on the stage of an inverted fluorescence microscope (Nikon TE300) and perfused with sEBSS to remove unattached cells and excess dye. All experiments were performed at 25°C in a continuous flow of sEBSS, with a perfusion rate of 0.6 ml/minute. Fluorescence excitation was at 470 nm (OptoLED, Cairn, UK) and emission at 520 nm. Images were captured at 0.2 Hz except for localisation of signal initiation (2.5 Hz) using a 40 \times or 60 \times oil-immersion objective and an Andor Ixon 897 EMCCD camera controlled by iQ3 software (Andor Technology, Belfast). Stimuli were applied to the cells by inclusion in the perfusing medium. In experiments where valinomycin exposure was combined with modified $[\text{K}^+]_o$ the cells were maintained in standard sEBSS except during the period of exposure to valinomycin.

Analysis of images and background correction was done using iQ3 software. Regions of interest were drawn around the required area(s) and the background subtracted. Average intensity was obtained for each area. Analysed and plotted data refer to the signal obtained from the posterior head/neck except

where more detailed regional analysis is described. For comparison of fluorescence in multiple regions within the sperm, cells with an adequately-immobilised flagellum were selected for analysis in order that fluorescence could be recorded from regions of interest in the flagellum as well as from the sperm neck and post-acrosomal head. Raw intensity values were imported into Microsoft Excel and normalized by calculating percentage change in fluorescence (ΔF) using the equation:

$$\Delta F = [(F - F_{rest})/F_{rest}] \times 100\%$$

where ΔF is the percentage change in fluorescence intensity at time t , F is fluorescence intensity at time t and F_{rest} is the mean of ≥ 10 determinations of F during the control period before application of P4.

Repetitive $[Ca^{2+}]_i$ activity (oscillations) induced by 3 μM P4 stimulation was analysed for amplitude and frequency. Oscillation (and P4-induced transient) amplitudes were calculated, for each event, as the increment in ΔF (calculated as the difference between the ΔF values at the signal peak and immediately before onset of the signal). For each cell mean amplitude for the experimental (treatment) period was then calculated and either normalised to the equivalent mean for the preceding control period or expressed a % of the amplitude of the initial P4-induced transient. Background $[Ca^{2+}]_i$ noise or ‘ripples’ with amplitude $< 20\%$ of the amplitude of the preceding P4-induced transient peak were not considered oscillations. Latency of $[Ca^{2+}]_i$ signals in the sperm head and neck (compared to the proximal flagellum) was estimated directly from the traces by identifying the start of the rising phase of the fluorescence signal (inflexion in the fluorescence trace) in each of the different regions. Oscillation frequency was estimated by counting the number of $[Ca^{2+}]_i$ spikes and dividing by time. Oscillation duration was assessed by taking the period between initiation and complete decay of the $[Ca^{2+}]_i$ signal.

Calculation of effective dose of RU1968. We have previously reported that compounds applied by superfusion may be present in the imaging chamber at concentrations significantly lower than that applied to the perfusion inflow (Brown, et al., 2017). In pilot experiments, the potency of RU1968 was lower than previously reported (Rennhack, et al., 2018). We therefore carried out parallel

experiments to compare the efficacy of RU1968 (1, 10, 20 and 30 μM), when applied by superfusion of the imaging chamber and when used in a static incubation chamber (multiwell plate; Achikanu, et al., 2018), in blocking the $[\text{Ca}^{2+}]_i$ transient induced by 3 μM P4. Data obtained with each method were fitted with a four parameter logistic regression model ($Y = \text{min} + (\text{max} - \text{min}) / (1 + (X / \text{IC}_{50})^{\text{Hill coefficient}})$) using <https://mycurvefit.com/>.

When RU1968 was applied by addition to a static chamber the calculated IC_{50} was 6.9 μM , similar to the previously reported value of 5.5 μM (Rennhack, et al., 2018). However, when applied by superfusion IC_{50} was 18.4 μM (fig S1). From the fitted curves we estimate that effective concentrations achieved by adding 10 and 30 μM RU1968 to the perfusing medium were 4.8 and 11.0 μM respectively (fig S1).

Statistics. Data were assessed for normality using the Anderson-Darling method and tested accordingly. Chi-square test was used for categorical variables (with adjustment for multiple testing as appropriate). t-test (paired or independent), Mann-Whitney or Wilcoxon test, with adjustment for multiple testing as appropriate, were used for continuous variables. ANOVA or Kruskal-Wallis test was used for comparing multiple groups.

Results

Following stimulation with 3 μM P4, repetitive $[\text{Ca}^{2+}]_i$ activity (repetitive spiking or oscillatory activity) was observed in a sub-population of human sperm, occurrence varying between samples (10-50% of cells). Mean amplitude was $53.2 \pm 1.3\%$ of the preceding P4-induced transient (310 oscillations in 101 cells) and mean frequency was 0.46 ± 0.02 cycles.min⁻¹ (101 cells).

$[\text{Ca}^{2+}]_i$ oscillations initiate in the flagellum. In order to investigate how repetitive Ca^{2+} signals are generated, we first assessed their point of origin and spread within the sperm cell. Images were captured at 2.5 Hz and regions of interest were analysed in the head, neck region/midpiece and in the principal piece of the flagellum at points approximately 1/3 (≈ 15 μM ; proximal) and 2/3 (≈ 30 μm , distal) of the distance from midpiece to tip. Examination of traces obtained from the different regions of interest showed that elevation of $[\text{Ca}^{2+}]_i$ consistently initiated in the principal piece. Start time of the $[\text{Ca}^{2+}]_i$ signal in the proximal and distal flagellum were similar ($P > 0.1$) but the signals in the neck and head occurred with a latency of 1.47 ± 0.14 and 2.21 ± 0.20 s respectively, compared to the proximal flagellum ($P < 0.001$; 21 cells; Wilcoxon; fig 1a,b, video 1, fig S2a). Latency of signal spread from the principal piece to the head showed no dependence on the order of occurrence in the oscillation series (first 4 oscillations, $P > 0.8$; Kruskal-Wallis with post hoc comparison). For comparison, we also examined the preceding P4-induced $[\text{Ca}^{2+}]_i$ transient. The transient initiated in the principal piece with latencies to the neck and head of 1.40 ± 0.34 s ($n=18$ cells; $p > 0.8$ compared to oscillations) and 2.30 ± 0.35 s respectively ($n=21$ cells; $P > 0.8$ compared to oscillations; fig 1b, video 2; fig S2a).

Signal amplitude (increment in ΔF calculated as the difference between the ΔF values at the signal peak and immediately before onset of the signal) was also assessed at the four regions of interest. Fluorescence increments in the head and neck were significantly greater than in the flagellum ($P = 2.2 \times 10^{-5}$; ANOVA with Tukey post hoc comparison; fig 1c). Equivalent analysis of the amplitude of the initial P4-induced $[\text{Ca}^{2+}]_i$ transient showed that though the mean amplitude was slightly larger

at the head and neck than in the flagellum, there was no significant difference between regions within the cell ($P=0.67$, ANOVA; fig 1d)

Since $[Ca^{2+}]_i$ oscillations originate in the principal piece of the flagellum, the most likely source for this initial Ca^{2+} increase is influx at the plasma membrane. In previous studies we showed that $[Ca^{2+}]_i$ oscillations are rapidly terminated in saline with no added Ca^{2+} and buffered with 2 mM EGTA, suggesting that mobilisation of stored Ca^{2+} cannot sustain oscillations in the absence of Ca^{2+} influx. However, when Ca^{2+} was simply omitted from the saline (' Ca^{2+} free' - $[Ca^{2+}] < 5 \mu M$), oscillations persisted and were often enlarged, primarily because the troughs between peaks approached more nearly to resting $[Ca^{2+}]_i$ (Harper, et al., 2004). Since EGTA buffered saline may cause rapid depletion of stored Ca^{2+} (Bedu-Addo et al., 2007), the inhibitory effect of EGTA-buffered saline on oscillations cannot be considered proof that Ca^{2+} -influx is essential, leaving the possibility that repeated mobilisation of stored Ca^{2+} (and consequent oscillation of $[Ca^{2+}]_i$) can occur under conditions of greatly reduced Ca^{2+} influx. To investigate this further we observed the effect on oscillations of prolonged superfusion with ' Ca^{2+} -free' saline. As described previously (Harper, et al., 2004), after a brief hiatus, oscillations persisted in cells superfused with ' Ca^{2+} free' saline. However, after a further 5-15 min both rise and decay time of oscillations slowed and $[Ca^{2+}]_i$ eventually settled at a level close to or below the initial resting value (fig 1e blue shading; mean time to arrest= 12.3 ± 0.5 min; max = 22.7 min; $n=51$ cells from 3 experiments). Subsequent addition of EGTA caused an immediate fall in $[Ca^{2+}]_i$ to very low levels (fluo4 fluorescence was 30-80% below the initial resting value; fig 1e grey shading). As reported previously, $[Ca^{2+}]_i$ did not recover when EGTA was removed (Bedu-Addo et al., 2007, Harper, et al., 2004) but upon return to standard sEBSS $[Ca^{2+}]_i$ immediately rose to a plateau level that exceeded the amplitude of the P4-induced transient (20-200% greater).

Hyperpolarisation of V_m inhibits $[Ca^{2+}]_i$ oscillations. Since $[Ca^{2+}]_i$ oscillations originate in the flagellum, where Ca^{2+} signals will be generated by influx at the plasma membrane, we investigated the possible involvement of V_m in regulating membrane Ca^{2+} channels, by using the K^+ ionophore valinomycin (1 μM) to 'clamp' the membrane at E_K (~ -78 mV assuming $[K^+]_i=120$ mM). Valinomycin uncouples mitochondria (e.g. Felber and Brand, 1982, Salvioli, et al., 2000) and can

cause a small increase in $[Ca^{2+}]_i$ in human sperm, but we have shown previously that mitochondrial uncouplers do not inhibit generation of $[Ca^{2+}]_i$ oscillations in human sperm (Harper, et al., 2004, Machado-Oliveira, et al., 2008). We first assessed the efficacy of valinomycin by directly observing V_m of cells held in whole cell current clamp. In cells bathed in standard sEBSS ($[K^+]=5.4$ mM), mean V_m of dialysed cells (1 min after breakthrough into whole cell recording mode) was -42.7 ± 3.7 mV ($n=6$). Upon exposure to valinomycin, V_m rapidly hyperpolarised (fig 2a), settling at -72.5 ± 1.6 mV within ≈ 2 min (fig 2). Subsequent change to valinomycin saline containing 100 mM K^+ induced a rapid (within 1 min) shift to a stable value of -9.0 ± 1.5 mV, which could be reversed by return to standard saline (fig 2a). These values fall close to those for E_K predicted by the Nernst equation (-76.8 mV and -3.3 mV) for the known intra- and extracellular K^+ concentrations (fig S3).

When cells bathed in standard (5.4 mM K^+) saline were exposed to valinomycin we saw a small, sustained increase in $[Ca^{2+}]_i$, as observed previously (Fraire-Zamora and Gonzalez-Martinez, 2004, Linares-Hernandez, et al., 1998). Subsequent application of 3 μ M P4 induced a $[Ca^{2+}]_i$ transient similar to that observed in parallel controls without valinomycin pretreatment (fig 3a,b; $p=0.95$ $n=8$; paired t), indicating that this saturating dose of P4 can effectively gate CatSper in cells clamped to ≈ -75 mV. However, following the initial transient, the occurrence of $[Ca^{2+}]_i$ oscillations was negligible until washout of valinomycin, upon which many cells became active, indicating that oscillations, unlike the initial transient, may be inhibited by hyperpolarisation of V_m (fig 3c). To further assess this effect we reversed the order of treatment, first stimulating cells with P4 to induce an ‘oscillating’ sub-population (activity with amplitude $\geq 20\%$ of the preceding P4-induced transient), then exposing the cells to valinomycin in the continued presence of P4. Superfusion with 1 μ M valinomycin rapidly suppressed activity (fig 4a, video 3, fig S2b), oscillations persisting in only 18.3% of the oscillating sub-population (47/257 cells in 16 experiments) after hyperpolarisation of V_m , compared to 99% (147/149) in control experiments (fig 5a; $p=5 \times 10^{-55}$; chi square). In 7 experiments the valinomycin was washed off after 15 min exposure and recording was continued for a further 15 min. Of 94 cells where valinomycin caused arrest of oscillations, 62 (66%) restarted, activity appearing within ≈ 5 min of valinomycin washout (fig 4a, video 3, fig S2b). In those cells where activity persisted in the

presence of valinomycin, both the amplitude and frequency of the $[Ca^{2+}]_i$ signals were reduced (fig 4a). To quantify this effect we selected 22 cells (from 3 experiments) and analysed the characteristics of the oscillations that persisted in the presence of valinomycin. Upon application of valinomycin both amplitude and frequency of the persisting oscillations were reduced to approximately one third of their values in the preceding control period ($P \leq 0.0001$; Mann-Whitney and paired t respectively; fig 5b,c).

Effect of valinomycin treatment is dependent on E_K . To, assess the importance of hyperpolarisation in the observed inhibition of $[Ca^{2+}]_i$ oscillations by valinomycin, we repeated the experiments, applying valinomycin in the presence of 25 mM K^+ ($E_K = -39.5$ mV with $[K^+]_i = 120$ mM; similar to the measured resting potential) and 100 mM K^+ (conditions which should fully depolarise V_m ; $E_K = -4.6$ mV with $[K^+]_i = 120$ mM). When co-applied with 25 mM K^+ the inhibition by valinomycin was still observed (video 4, fig S2c) but the effect of significantly ameliorated, almost half of oscillating cells (58/117 in 3 experiments) remaining active (figs 4b, 5a). When valinomycin was co-applied with 100 mM K^+ there was a more marked increase in underlying $[Ca^{2+}]_i$ (compare figs 4a and 4c) and the inhibitory effect on $[Ca^{2+}]_i$ oscillations was further reduced, activity persisting in over 75% (86/114) of oscillating cells (figs 4c, 5a, video 5, fig S2d). Comparison across the three conditions confirmed that the efficacy of valinomycin in suppressing activity was highly dependent on $[K^+]_o$ ($P = 10^{-25}$; chi-square).

Examination of the characteristics of oscillations in those cells where spontaneous activity persisted in the presence of valinomycin showed that the effects of treatment on amplitude and (more particularly) frequency were similarly dependent on the extracellular K^+ concentration. As in standard sEBSS, exposure to valinomycin reduced both the amplitude and frequency of oscillations, but these effects were dependent on $[K^+]_o$, being ameliorated as E_K was shifted to more positive values (fig 4; fig 5b,c; $P = 0.003$ (Kuskal-Wallis) and $P = 10^{-6}$ (ANOVA) for amplitude and frequency respectively). When valinomycin was washed out (combined with a return to standard sEBSS) spontaneous activity was able to recover. In cells exposed to valinomycin in 25 mM and 100 mM K^+ saline, oscillations restarted in 45/59 (76%) and 12/28 (43%) of previously oscillating cells respectively. Following

valinomycin/100 mM K⁺ treatment the delay before activity resumed was noticeably longer (typically ≥15 min; fig 4c).

Blockade of CatSper reversibly inhibits [Ca²⁺]_i oscillations. CatSper, the primary Ca²⁺ channel of human sperm, is voltage sensitive and is localised to the sperm flagellum (Lishko, et al., 2011). To assess the involvement of CatSper in generation of oscillations, we tested the effect of RU1968, a ‘specific’ blocker which does not affect pHi and has limited effects on sperm K⁺ conductance (Rennhack, et al., 2018). Sperm were first exposed to P4 to establish oscillations in a sub-population of cells, then RU1968 was applied, in the continued presence of P4.

At an estimated concentration of 11 μM (see methods), spontaneous activity was rapidly and completely inhibited in the great majority of oscillating cells, only 6.9% of the oscillating cells remaining active (4/58 cells in 3 experiments; fig. 6a, 7a, video 6, fig S2e), compared to 98.9% (88/89) in parallel controls exposed to 0.3% DMSO (p=10⁻²⁹; Chi-square). It was noticeable that, unlike the effect of valinomycin, background [Ca²⁺]_i noise or ‘ripples’ (amplitude <20%) were also largely suppressed (compare figs 4a and 6a). Each of the 4 cells in which activity persisted generated a single transient during the 10 min period of exposure to RU1968. Amplitude of these [Ca²⁺]_i signals varied from 20-100% of those recorded during the preceding control period. Upon washout of the drug (exposure time=10 min), spontaneous activity recovered in 80% (43/54) of the cells where treatment had caused arrest of activity.

Exposure to an estimated concentration of 4.8 μM RU1968 caused a transient increase in [Ca²⁺]_i in all cells, which varied greatly in amplitude and decayed within 3-5 min (fig 6b, video , fig S2f; compare to 11 μM [figs 6a, S2e] where immediate suppression of activity occurs). Oscillations persisted in 64.3% of the cells that were previously active (83/129 cells, 3 experiments; fig 6b, 7a; P=8*10⁻¹⁴ compared to 11 uM) whereas in parallel control experiments oscillations persisted in 98.3% of cells (59/60 cells; p=10⁻⁶; Chi-square). In those cells that continued to generate spontaneous activity the characteristics of the [Ca²⁺]_i signals were clearly modified (fig 6b, video 7, fig S2f). The frequency of

persisting oscillations was reduced by almost 50% (fig 7b; $P < 10^{-16}$; Mann-Whitney) and both the amplitude of oscillations (fig 7c) and their duration (fig 7d) were significantly increased compared to the preceding control period ($P = 1.5 \times 10^{-5}$, paired t and $P < 10^{-16}$, Mann-Whitney, respectively). When RU1968 was washed out of the recording chamber spontaneous activity recovered in 72% (33/46) of the cells where oscillations had been inhibited ($P = 0.73$ compared to 11 μM ; chi square). In approximately half (20/38) of those cells where P4 treatment had failed to induce significant oscillations (defined as $\geq 20\%$ of the preceding P4-induced transient; see methods), the transient $[\text{Ca}^{2+}]_i$ increase that occurred upon application of 4.8 μM RU1968 was followed by second large, slow oscillation (fig S4). Repetitive activity persisted after washout of RU1968 in 8 of these cells.

The KSper blocker quinidine inhibits $[\text{Ca}^{2+}]_i$ oscillations. Quinidine (300 μM) blocked KSper currents in human sperm by $\approx 90\%$ (Mansell, et al., 2014) and potently blocks mouse Slo3 (KSper) channels (Tang et al, 2010). Application of 300 μM quinidine to cells in which oscillations had previously been established by exposure to P4 resulted in complete block of $[\text{Ca}^{2+}]_i$ activity (36/36 cells; fig 6c; $P = 1.7 \times 10^{-30}$ compared to control, chi-square). Similarly to treatment with RU1968, $[\text{Ca}^{2+}]_i$ noise or ‘ripples’ (amplitude $< 20\%$) were also suppressed in most cells (fig 6c). Upon washout (exposure time=10 min) there was an immediate $[\text{Ca}^{2+}]_i$ spike, even in those cells in which oscillations were not previously observed, but restart of oscillations occurred in only 6/36 cells (16.7%), significantly lower than the responses seen under any other of the treatments tested ($P < 0.05$; chi square).

Discussion

We and others have reported the occurrence of repetitive $[Ca^{2+}]_i$ elevations, in human sperm, that contribute to regulation of key sperm functions (Bedu-Addo et al., 2007, Harper, et al., 2004, Machado-Oliveira, et al., 2008, Mata-Martinez, et al., 2018, Sanchez-Cardenas, et al., 2014). Here we have further investigated the mechanisms by which these signals are generated.

Oscillations originate in the flagellum. Consistent with previous reports (Servin-Vences, et al., 2012; Alasmari, et al., 2013), the initial P4-induced $[Ca^{2+}]_i$ transient initiated in the flagellar principal piece. Oscillations behaved similarly, propagating from the flagellum to the head/neck region with kinetics similar to those of the initial transient. Oscillation amplitude measured at the sperm head/neck, was significantly greater than at the flagellum. This observation is consistent with mobilisation of a secondary Ca^{2+} source in this region (Bedu-Addo et al., 2007; Olson, et al., 2010, Publicover, 2017). However, this must be interpreted cautiously. A non-ratiometric dye was used in this study and apparent regional variation in the normalised responses might be due to other factors, such as differences in resting $[Ca^{2+}]_i$ between flagellum and sperm head.

Oscillations are dependent on V_m . Manipulation of V_m with valinomycin, (fig 2), had no effect on the P4-induced $[Ca^{2+}]_i$ transient, possibly because of the saturating concentration of P4 used in this study. In contrast, oscillations were strongly suppressed by valinomycin-induced hyperpolarisation. This inhibition was ameliorated when V_m was set to more +ve potentials. If fluctuation of V_m plays a role in P4-induced $[Ca^{2+}]_i$ oscillation (see below), limited cyclic regulation of V_m must persist in these cells, despite the presence of valinomycin. We conclude that initiation of oscillations in the flagellar principal piece is regulated by or sensitive to V_m .

Blockade of CatSper and KSper inhibits oscillations. Since $[Ca^{2+}]_i$ oscillations require extracellular Ca^{2+} (fig. 1e) we investigated the importance of CatSper. The CatSper blocker RU1968 ($IC_{50} \approx 5 \mu M$) dose-dependently suppressed $[Ca^{2+}]_i$ oscillations. Though the drug also inhibits Slo3, this action is 15-fold less potent than CatSper block (Rennhack, et al., 2018). The effects of RU1968 reported here (particularly the lower dose estimated at $4.8 \mu M$) will reflect primarily its action on CatSper and we

therefore conclude that initiation of oscillations in the flagellum involves CatSper-mediated Ca^{2+} -influx. Intriguingly, where oscillations persisted in the presence of RU1968, their frequency was reduced but amplitude and duration were significantly increased. This may reflect resetting of the ‘oscillator’ in the flagellum due to reduced currents through CatSper, or might even be oscillatory behaviour of Ca^{2+} stores persisting after inhibition of Ca^{2+} influx.

Quinidine (300 μM), which blocks human KSper (Brenker, et al., 2014; Mansell, et al., 2014), was strikingly effective in arresting $[\text{Ca}^{2+}]_i$ oscillations. However, in addition to its action on KSper, 300 μM quinidine blocks CatSper currents (Zeng et al., 2011; Mansell, et al., 2014) an effect that might underlie our observations. However, it is noteworthy that recovery of oscillations following washout of RU1968 was rapid (80% of silenced cells recovered) whereas no recovery was seen with quinidine (compare figs 6a and 6c). In whole cell patch clamp recordings the effects of quinidine on CatSper currents washed out rapidly (30 s) whereas KSper recovered more slowly (3-4 min; Mansell, et al., 2014), which might underlie this observation.

Generation of $[\text{Ca}^{2+}]_i$ oscillations in human sperm. The data presented here do not allow us to develop a clear model for the mechanism underlying the generation of repetitive $[\text{Ca}^{2+}]_i$ activity in the flagellum of P4-stimulated human sperm. However, since (i) their generation is dependent on V_m and requires activity of CatSper and probably KSper, (ii) CatSper opening is increased by depolarisation of V_m , (iii) KSper, which regulates V_m , is stimulated by elevated $[\text{Ca}^{2+}]_i$ (Brenker, et al., 2014, Brown, et al., 2016; Mannowetz, et al., 2013), oscillations could involve a feedback loop in which $[\text{Ca}^{2+}]_i$ is elevated during V_m depolarisation, leading to activation of KSper and consequent repolarisation. Such V_m -regulated, cyclic Ca^{2+} influx has been described in a diverse range of cell types, occurring either as periodic action potential bursts (Cornelisse, et al., 2001, Gorman and Thomas, 1978, Schlegel, et al., 1987) or repeated depolarising excursions of V_m (Ferrier, et al., 1987, Lopez, et al., 2014). However, some aspects of P4-induced oscillations reported here and elsewhere appear inconsistent with this simple model and require further investigation. Firstly, in the presence of valinomycin any effects of KSper currents on V_m will be damped, both because of the increased constitutive K^+ ‘leak’ and because valinomycin sets V_m at or close to E_K (figure S3). Though most

oscillations are inhibited, some cells, particularly with $[K^+]_o = 100$ mM, continue to generate small $[Ca^{2+}]_i$ oscillations. Secondly, we observed previously that following stimulation with P4, $\approx 50\%$ of oscillating cells continue to oscillate (or restart) after P4 washout (Harper et al, 2004), even though P4-withdrawal will cause a +ve shift in voltage sensitivity of CatSper (Lishko, et al., 2011).

Other potential causes of/contributors to generation of $[Ca^{2+}]_i$ oscillations include regulation of CatSper activity by oscillation of pH_i . Feedback mechanisms involving fluctuations of V_m and pH_i have been proposed to underlie the trains of $[Ca^{2+}]_i$ spikes that occur in the flagellum of sea urchin sperm (Priego-Espinosa, et al., 2020, Wood, et al., 2003). These $[Ca^{2+}]_i$ signals, similarly to those investigated here, initiate in the flagellum and are inhibited by manipulation of V_m , though their kinetics are strikingly different (Wood, et al., 2003). In human sperm the voltage dependent H^+ channel Hv1 is expressed (Lishko, et al., 2010) and thus depolarisation of V_m might lead indirectly to CatSper activation via H^+ efflux and cytoplasmic alkalinisation (Lishko and Kirichok, 2010). However, human KSper shows low sensitivity to pH_i (Brenker, et al., 2014) and capacitation and incubation at acid pH ($pH_o=6.5$), conditions which would significantly reduce the value of pH_i that might be achieved upon activation of Hv1, increased both the occurrence (% cells) and size of $[Ca^{2+}]_i$ oscillations in human sperm (Mata-Martinez, et al., 2018).

$[Ca^{2+}]_i$ oscillations and fertility. With regard to the potential clinical significance of these observations, a recent study on cells used for IVF showed that the occurrence of oscillating cells was low in samples that failed to fertilise. In particular, the proportion of samples where no oscillating cells were observed was significantly greater in non-fertilising samples than in samples from patients where fertilisation was successful (Kelly, et al., 2018). This suggests that failure of oscillations themselves, or of the physiological processes that generate them, may underlie some instances of idiopathic infertility. Oscillations appear to be involved in regulation of flagellar activity and acrosome reaction (see introduction) so their failure could well result in a reduced chance of fertilisation, both *in vivo* and in IVF. With regard to the underlying physiological mechanisms, complete loss of CatSper expression or function appears to be rare, even in sperm of subfertile men (Brown, et al., 2019), but either reduced functional expression of CatSper (Tamburrino, et al., 2015;

Marchiani, et al., 2017) or impaired regulation of V_m (Brown et al., 2016) might result in failure to generate $[Ca^{2+}]_i$ oscillations. Detection of the occurrence of oscillations as a component of routine semen assessment clearly is impractical, since they can be observed only by time-lapse fluorescence imaging, but further studies on their generation, regulation and functional significance may well throw light on key aspects of the fertilisation process.

Authors' roles

E.T., S.G. and E.M-M. carried out the laboratory work. E.T., S.G. E.M-M. and S.P. analysed the data. All authors contributed to writing and/or editing of the ms.

Funding

ET-N was in receipt of a postgraduate scholarship from the CAPES Foundation (Ministry of Education, Brazil).

Conflict of interest

The authors have no conflicts of interest.

References

- Achikanu C, Pendekanti V, Teague R, Publicover S. Effects of pH manipulation, CatSper stimulation and Ca^{2+} -store mobilization on $[\text{Ca}^{2+}]_i$ and behaviour of human sperm. *Hum Reprod* 2018;33: 1802-1811.
- Alasmari W, Costello S, Correia J, Oxenham SK, Morris J, Fernandes L, Ramalho-Santos J, Kirkman-Brown J, Michelangeli F, Publicover S *et al.* Ca^{2+} signals generated by CatSper and Ca^{2+} regulate different behaviours in human sperm. *J Biol Chem* 2013;288: 6248-6258.
- Bedu-Addo K, Barratt CL, Kirkman-Brown JC, Publicover SJ. Patterns of $[\text{Ca}^{2+}]_i$ mobilization and cell response in human spermatozoa exposed to progesterone. *Dev Biol* 2007;302: 324-332.
- Berridge MJ, Bootman MD, Roderick HL. Calcium signalling: dynamics, homeostasis and remodelling. *Nat Rev Mol Cell Biol* 2003;4: 517-529.
- Berridge MJ, Cobbold PH, Cuthbertson KS. Spatial and temporal aspects of cell signalling. *Philos Trans R Soc Lond B Biol Sci* 1988;320: 325-343.
- Brenker C, Zhou Y, Muller A, Echeverry F, Trotschel C, Poetsch A, Xia X, Bonigk W, Lingle C, Kaupp U *et al.* Slo3 in human sperm - a K^+ channel activated by Ca^{2+} *ELife* 2014;3:e01438.
- Brown SG, Costello S, Kelly MC, Ramalingam M, Drew E, Publicover SJ, Barratt CLR, Martins Da Silva S. Complex CatSper-dependent and independent $[\text{Ca}^{2+}]_i$ signalling in human spermatozoa induced by follicular fluid. *Hum Reprod* 2017;32: 1995-2006.
- Brown SG, Publicover SJ, Barratt CL, Martins da Silva S. Human sperm ion channel (dys)function: implications for fertilization. *Human Reproduction Update* 2019; 25, 758–776.
- Brown SG, Publicover SJ, Mansell SA, Lishko PV, Williams HL, Ramalingam M, Wilson SM, Barratt CL, Sutton KA, Martins Da Silva S. Depolarization of sperm membrane potential is a common feature of men with subfertility and is associated with low fertilization rate at IVF. *Hum Reprod* 2016;31: 1147-1157.
- Cai X, Clapham DE. Evolutionary genomics reveals lineage-specific gene loss and rapid evolution of a sperm-specific ion channel complex: CatSper and CatSperbeta. *PLoS One* 2008;3: e3569.

479 Cornelisse LN, Scheenen WJ, Koopman WJ, Roubos EW, Gielen SC. Minimal model for intracellular
 480 calcium oscillations and electrical bursting in melanotrope cells of *Xenopus laevis*. *Neural Comput*
 481 2001;13: 113-137.
 482 Correia J, Michelangeli F, Publicover S. Regulation and roles of Ca^{2+} stores in human sperm.
 483 *Reproduction (Cambridge, England)* 2015;150: R65-76.
 484 Costello S, Michelangeli F, Nash K, Lefievre L, Morris J, Machado-Oliveira G, Barratt C, Kirkman-
 485 Brown J, Publicover S. Ca^{2+} stores in sperm: their identities and functions. *Reproduction* 2009;138:
 486 425-437.
 487 Darszon A, Nishigaki T, Beltran C, Trevino CL. Calcium channels in the development, maturation,
 488 and function of spermatozoa. *Physiol Rev* 2011;91: 1305-1355.
 489 Felber SM, Brand MD. Valinomycin can depolarize mitochondria in intact lymphocytes without
 490 increasing plasma membrane potassium fluxes. *FEBS Lett* 1982;150: 122-124.
 491 Ferrier J, Ward-Kesthely A, Homble F, Ross S. Further analysis of spontaneous membrane potential
 492 activity and the hyperpolarizing response to parathyroid hormone in osteoblastlike cells. *J Cell*
 493 *Physiol* 1987;130: 344-351.
 494 Fraire-Zamora JJ, Gonzalez-Martinez MT. Effect of intracellular pH on depolarization-evoked
 495 calcium influx in human sperm. *Am J Physiol Cell Physiol* 2004;287: C1688-1696.
 496 Gorman AL, Thomas MV. Changes in the intracellular concentration of free calcium ions in a pace-
 497 maker neurone, measured with the metallochromic indicator dye arsenazo III. *J Physiol* 1978;275:
 498 357-376.
 499 Guerrero A, Nishigaki T, Carneiro J, Yoshiro T, Wood CD, Darszon A. Tuning sperm chemotaxis by
 500 calcium burst timing. *Dev Biol* 2010;344: 52-65.
 501 Harper CV, Barratt CL, Publicover SJ. Stimulation of human spermatozoa with progesterone
 502 gradients to simulate approach to the oocyte. Induction of $[\text{Ca}^{2+}]_i$ oscillations and cyclical
 503 transitions in flagellar beating. *J Biol Chem* 2004;279: 46315-46325.
 504 Kaupp UB, Kashikar ND, Weyand I. Mechanisms of sperm chemotaxis. *Annu Rev Physiol* 2008;70:
 505 93-117.

506 Kelly MC, Brown SG, Costello SM, Ramalingam M, Drew E, Publicover SJ, Barratt CLR, Martins
 507 Da Silva S. Single-cell analysis of $[Ca^{2+}]_i$ signalling in sub-fertile men: characteristics and relation to
 508 fertilization outcome. *Hum Reprod* 2018;33: 1023-1033.
 509 Linares-Hernandez L, Guzman-Grenfell AM, Hicks-Gomez JJ, Gonzalez-Martinez MT. Voltage-
 510 dependent calcium influx in human sperm assessed by simultaneous optical detection of intracellular
 511 calcium and membrane potential. *Biochim Biophys Acta* 1998;1372: 1-12.
 512 Lishko PV, Botchkina IL, Fedorenko A, Kirichok Y. Acid extrusion from human spermatozoa
 513 is mediated by flagellar voltage-gated proton channel. *Cell* 2010;140: 327–337,
 514 Lishko PV, Botchkina IL, Kirichok Y. Progesterone activates the principal Ca^{2+} channel of human
 515 sperm. *Nature* 2011;471: 387-391.
 516 Lishko PV, Kirichok Y. The role of Hv1 and CatSper channels in sperm activation. *J Physiol*
 517 2010;588: 4667-4672.
 518 Lopez MG, Artalejo AR, Garcia AG, Neher E, Garcia-Sancho J. Veratridine-induced oscillations of
 519 cytosolic calcium and membrane potential in bovine chromaffin cells. *J Physiol* 1995;482 (Pt 1): 15-
 520 27.
 521 Machado-Oliveira G, Lefievre L, Ford C, Herrero MB, Barratt C, Connolly TJ, Nash K, Morales-
 522 Garcia A, Kirkman-Brown J, Publicover S. Mobilisation of Ca^{2+} stores and flagellar regulation in
 523 human sperm by S-nitrosylation: a role for NO synthesised in the female reproductive tract.
 524 *Development* 2008;135: 3677-3686.
 525 Mannowetz N, Naidoo N, Choo S-AS, Smith JF, Lishko PV. Slo1 is the principal potassium channel of
 526 human spermatozoa. *eLife* 2013; PMID: 24137539 DOI: 10.7554/eLife.01009
 527 Mansell SA, Publicover SJ, Barratt CL, Wilson SM. Patch clamp studies of human sperm under
 528 physiological ionic conditions reveal three functionally and pharmacologically distinct cation
 529 channels. *Mol Hum Reprod* 2014; 20: 392-408.
 530 Marchiani S, Tamburrino L, Benini F, Fanfani L, Dolce R, Rastrelli G, Maggi M, Pellegrini S, Baldi
 531 E. Chromatin Protamination and Catsper Expression in Spermatozoa Predict Clinical Outcomes after
 532 Assisted Reproduction Programs. *Sci Rep* 2017 7:15122.

533 Mata-Martinez E, Darszon A, Trevino CL. pH-dependent Ca^{2+} oscillations prevent untimely
534 acrosome reaction in human sperm. *Biochem Biophys Res Commun* 2018;497: 146-152.

535 Mizutani H, Yamamura H, Muramatsu M, Kiyota K, Nishimura K, Suzuki Y, Ohya S, Imaizumi Y.
536 Spontaneous and nicotine-induced Ca^{2+} oscillations mediated by Ca^{2+} influx in rat pinealocytes. *Am J*
537 *Physiol Cell Physiol* 2014;306: C1008-1016.

538 Nash K, Lefievre L, Peralta-Arias R, Morris J, Morales-Garcia A, Connolly T, Costello S, Kirkman-
539 Brown JC, Publicover SJ. Techniques for imaging Ca^{2+} signaling in human sperm. *J Vis Exp* 2010:
540 doi:pii: 1996. 1910.3791/1996.

541 Olson SD, Suarez SS, Fauci LJ. A model of CatSper channel mediated calcium dynamics in
542 mammalian spermatozoa. *Bull Math Biol* 2010;72: 1925-1946.

543 Priego-Espinosa DA, Darszon A, Guerrero A, Gonzalez-Cota AL, Nishigaki T, Martinez-Mekler G,
544 Carneiro J. Modular analysis of the control of flagellar Ca^{2+} -spike trains produced by CatSper and
545 Ca_v channels in sea urchin sperm. *PLoS Comput Biol* 2020;16: e1007605.

546 Publicover S. Regulation of Sperm Behaviour: The Role(s) of $[\text{Ca}^{2+}]_i$ Signalling. In De Jonge CJD,
547 Barratt. CLR (ed) *The Sperm Cell, Second Edition*. 2017. Cambridge University Press, Cambridge
548 UK, pp. 126-142.

549 Publicover S, Harper CV, Barratt C. $[\text{Ca}^{2+}]_i$ signalling in sperm--making the most of what you've got.
550 *Nat Cell Biol* 2007;9: 235-242.

551 Ren D, Navarro B, Perez G, Jackson AC, Hsu S, Shi Q, Tilly JL, Clapham DE. A sperm ion channel
552 required for sperm motility and male fertility. *Nature* 2001;413: 603-609.

553 Rennhack A, Schiffer C, Brenker C, Fridman D, Nitao ET, Cheng YM, Tamburrino L, Balbach M,
554 Stolting G, Berger TK *et al*. A novel cross-species inhibitor to study the function of CatSper Ca^{2+}
555 channels in sperm. *Br J Pharmacol* 2018;175: 3144-3161.

556 Salvioli S, Barbi C, Dobrucki J, Moretti L, Pinti M, Pedrazzi J, Paziienza TL, Bobyleva V, Franceschi
557 C, Cossarizza A. Opposite role of changes in mitochondrial membrane potential in different apoptotic
558 processes. *FEBS Lett* 2000;469: 186-190.

559 Sanchez-Cardenas C, Servin-Vences MR, Jose O, Trevino CL, Hernandez-Cruz A, Darszon A.
 560 Acrosome reaction and Ca^{2+} imaging in single human spermatozoa: new regulatory roles of $[\text{Ca}^{2+}]_i$.
 561 *Biol Reprod* 2014;91: 67.
 562 Santi SM, Martínez-López P, de la Vega-Beltrán JL, Butler A, Alisio A, Darszon A, Salkoff L. The
 563 SLO3 sperm-specific potassium channel plays a vital role in male fertility. *FEBS Lett* 2010;
 564 584:1041–1046
 565 Schiffer C, Muller A, Egeberg DL, Alvarez L, Brenker C, Rehfeld A, Frederiksen H, Waschle B,
 566 Kaupp UB, Balbach M *et al.* Direct action of endocrine disrupting chemicals on human sperm. *EMBO*
 567 *Rep* 2014;15: 758-765.
 568 Schlegel W, Winiger BP, Mollard P, Vacher P, Wuarin F, Zahnd GR, Wollheim CB, Dufy B.
 569 Oscillations of cytosolic Ca^{2+} in pituitary cells due to action potentials. *Nature* 1987;329: 719-721.
 570 Seifert R, Flick M, Bonigk W, Alvarez L, Trotschel C, Poetsch A, Muller A, Goodwin N, Pelzer P,
 571 Kashikar ND *et al.* The CatSper channel controls chemosensation in sea urchin sperm. *The EMBO*
 572 *journal* 2015;34: 379-392.
 573 Servin-Vences MR, Tatsu Y, Ando H, Guerrero A, Yumoto N, Darszon A, Nishigaki T. A caged
 574 progesterone analog alters intracellular Ca^{2+} and flagellar bending in human sperm. *Reproduction*
 575 2012;144: 101-109.
 576 Smith JF, Syrityna O, Fellous M, Serres C, Mannowetz N, Kirichok Y, Lishko PV. Disruption of the
 577 principal, progesterone-activated sperm Ca^{2+} channel in a CatSper2-deficient infertile patient. *Proc*
 578 *Natl Acad Sci U S A* 2013;110: 6323-6328.
 579 Suarez SS. Control of hyperactivation in sperm. *Hum Reprod Update* 2008;14: 647-657.
 580 Tamburrino L, Marchiani S, Vicini E, Muciaccia B, Cambi M, Pellegrini S, Forti G, Muratori M,
 581 Baldi E. Quantification of CatSper1 expression in human spermatozoa and relation to functional
 582 parameters. *Hum Reprod* 2015; 30:1532-1544. doi: 10.1093
 583 Wood CD, Darszon A, Whitaker M. Speract induces calcium oscillations in the sperm tail. *J Cell Biol*
 584 2003;161: 89-101.
 585 World Health Organization DoRHAR. WHO laboratory manual for the examination and processing of
 586 human semen Fifth edition, 2010. World Health Organization.

587 Zeng X-H, Yang C, Kim ST, Lingle CJ, and Xia XM P Deletion of the Slo3 gene abolishes
588 alkalization-activated K⁺ current in mouse spermatozoa. *Proc Natl Acad Sci U S A* 2011;108: 5879–
589 5884
590
591

Figure legends

Figure 1. Site of initiation and $[Ca^{2+}]_o$ -sensitivity of $[Ca^{2+}]_i$ oscillations. a) $[Ca^{2+}]_i$ oscillation recorded in the principal piece (black trace) neck (red) and head (grey) of a single sperm. The $[Ca^{2+}]_i$ increase occurs first in the principal piece but signals in the neck and head are larger. Traces show % increase in fluo4 fluorescence intensity with respect to mean fluorescence before the progesterone (P4) stimulus (Δ fluorescence (%)). **b)** Mean latency of $[Ca^{2+}]_i$ responses in the neck (red) and head (grey) compared to those in the flagellum. Left panel shows mean \pm SEM (n=17 cells) for $[Ca^{2+}]_i$ oscillations, right panel shows mean \pm SEM (n=17 cells) for the preceding P4-induced $[Ca^{2+}]_i$ transients. Latencies of both oscillations and transients to the neck and head were similar ($P>0.2$) but all significantly exceeded zero (Wilcoxon) *** $p<0.001$. **c)** Mean amplitude \pm SEM (n=17 cells) of $[Ca^{2+}]_i$ oscillations recorded in the distal flagellum (black), sperm neck (red) and head (grey) normalised to amplitude in the proximal flagellum (black). Letters indicate statistically similar amplitudes. Amplitudes in the head and neck significantly exceeded those in the flagellum $P=2.2*10^{-5}$; ANOVA with Tukey post hoc comparison. **d)** Mean amplitude \pm SEM (n=17 cells) of P4-induced $[Ca^{2+}]_i$ transients recorded in the distal flagellum (black), sperm neck (red) and head (grey) normalised to amplitude in the proximal flagellum (black). Amplitudes did not differ significantly ($P=0.67$; ANOVA). **e)** Responses of 5 individual cells to stimulation with 3 μ M P4 (arrow), followed by superfusion with P4-containing 'Ca²⁺-free' saline ($[Ca^{2+}]<5 \mu$ M; blue shading) for 30 min. EGTA-buffered saline (calculated $[Ca^{2+}]=2.6*10^{-10}$ M; grey shading) was then superfused for 10 min before returning to 'Ca²⁺-free' saline and then to standard sEBSS. Note that oscillations arrest in 'Ca²⁺-free' saline, before application of EGTA buffer.

Figure 2. Valinomycin shifts membrane potential (V_m) to E_K . a) Current clamp recording of V_m in a single sperm. Grey shading shows periods of superfusion with 1 μ M valinomycin in standard (5.4 mM K⁺) saline. Red shading shows period of superfusion with 1 μ M valinomycin in depolarising (100 mM K⁺) saline. **b)** Recorded membrane potential (mean \pm SEM) for cells under control conditions

(black; n=6 cells), exposed to 1 μM valinomycin in standard (5.4 mM K^+) saline (grey; n=5 cells) and exposed to 1 μM valinomycin in depolarising (100 mM K^+) saline (red; n=5 cells).

Figure 3. Valinomycin does not inhibit the P4-induced $[\text{Ca}^{2+}]_i$ transient. **a)** Mean response to application of 3 μM P4 (arrow) in the presence of valinomycin (red trace) and in parallel control experiments (black trace), n=7 experiments for each condition. Baseline of the valinomycin trace has been adjusted to facilitate comparison with the control trace. **b)** Mean amplitude ($\pm\text{SEM}$) of the $[\text{Ca}^{2+}]_i$ transient recorded in the presence of valinomycin (red) and in its absence (black; n=8 experiments for each condition' $P=0.95$, paired t). **c)** Application 1 μM valinomycin (grey shading) causes a small, sustained increase in $[\text{Ca}^{2+}]_i$. Subsequent application of 3 μM P4 (arrow) induced a $[\text{Ca}^{2+}]_i$ transient but oscillations occurred only after washout of valinomycin. Oscillations arrested or paused upon washout of P4 (upward arrow). Responses of 4 separate cells shown. $[\text{K}^+]_o = 5.4$ mM throughout.

Figure 4. Effect of valinomycin on $[\text{Ca}^{2+}]_i$ oscillations. Cells were stimulated with 3 μM P4 (arrow) to induce oscillations then exposed to 1 μM valinomycin (shown by grey shading). **a)** $[\text{K}^+]_o = 5.4$ mM, (estimated $E_K = -78.1$ mV) . **b)** during valinomycin exposure $[\text{K}^+]_o$ was increased to 25 mM (estimated $E_K = -39.5$ mV). **c)** during valinomycin exposure $[\text{K}^+]_o$ was increased to 100 mM (estimated $E_K = -4.6$ mV). Each panel shows responses of 5 individual cells.

Figure 5. Effect of valinomycin on $[\text{Ca}^{2+}]_i$ oscillations depends on $[\text{K}^+]_o$. **a)** Proportion of oscillating cells in which activity was suppressed (shown by black shading) in the presence of 1 μM valinomycin varied with $[\text{K}^+]_o$ (5.4 mM, n=257 cells; 25 mM, n=117 cells and 100 mM, n=114 cells; $P=10^{-25}$; chi-square). **b)** Amplitude of oscillations that persisted in the presence of valinomycin varied with $[\text{K}^+]_o$. Bars show mean ($\pm\text{SEM}$) oscillation amplitude normalised to that during the control period (prior to valinomycin treatment, grey). 5.4 mM, n=9 cells; 25 mM, n=22 cells and 100 mM, n=22 cells. Asterisks indicate significant difference from control period, *** $p<0.001$, **** $p<0.0001$ (Paired t or Mann-Whitney). **c)** Frequency of oscillations that persisted in the presence of valinomycin varied with $[\text{K}^+]_o$. Bars show mean ($\pm\text{SEM}$) oscillation frequency normalised to that during the

control period (prior to valinomycin treatment; grey). 5.4 mM, n=9 cells; 25 mM, n=22 cells and 100 mM, n=22 cells. Asterisks indicate significant difference from control period, **** p<0.0001, (Paired-t or Mann-Whitney).

Figure 6. RU1968 and quinidine inhibit $[Ca^{2+}]_i$ oscillations. Cells were stimulated with 3 μ M progesterone (P4; arrow) to induce oscillations then exposed to RU1968 or quinidine (shown by grey shading). **a)** Effect of 11 μ M RU1968. **b)** Effect of 4.8 μ M RU1968. **c)** Effect of 300 μ M quinidine. Each panel shows responses of 5 individual cells.

Figure 7. Effect of RU1968 on incidence and characteristics of $[Ca^{2+}]_i$ oscillations. **a)** Proportion of cells in which oscillations were inhibited (shown by black shading) in the presence of 4.8 μ M (n=129 cells) and 11 μ M RU1968 (n=58 cells). **b)** Frequency of oscillations in cells in which activity persisted in the presence of 4.8 μ M RU1968 (red) was significantly decreased compared to preceding (control) period (grey; n=67 cells). **c)** Amplitude of oscillations in cells in which activity persisted in the presence of 4.8 μ M RU1968 (red) was significantly increased compared to preceding (control) period (grey n=67 cells). **d)** Duration of oscillations in cells in which activity persisted in the presence of 4.8 μ M RU1968 (red) was significantly increased compared to preceding (control) period (grey; n=73 cells). Asterisks indicate significant difference from control period, ****P<0.0001 (Paired-t or Mann-Whitney).

660

661 **Supplementary figure legends**

Figure S1. Effective dose of RU1968 is reduced in superfusion experiments. Dose-dependency of inhibition by RU1968 of the $[Ca^{2+}]_i$ transient induced by 3 μ M progesterone in static chamber experiments (red, IC₅₀=6.9 μ M) and imaging experiments in the superfusion chamber (black, IC₅₀=18.4 μ M). Points show mean \pm SEM of 3 or 4 experiments. Curve fitting and calculation of IC₅₀ were done using <https://mycurvefit.com/>. Arrows show estimation of effective concentrations applied in superfusion experiments.

Figure S2. Time-fluorescence plots for cells shown in videos 1-7. Arrows indicate time of application of 3 μM progesterone (P4). **Panel a** shows rising phase of P4-induced $[\text{Ca}^{2+}]_i$ transient (left ; video 1) and a subsequent $[\text{Ca}^{2+}]_i$ oscillation (right ; video 2) in the same cell. Black traces show responses in proximal flagellum, red traces show responses in head. Amplitudes are scaled (minimum to maximum) to facilitate comparison of time-course. **Panels b, c and d** show % increase in fluo4 fluorescence intensity with respect to mean fluorescence before the P4 stimulus (Δ fluorescence (%)) for the cells in videos 3, 4 and 5 respectively. Grey shading shows period of exposure to 1 μM valinomycin (panel b), 1 μM valinomycin with 25 mM K^+ (panel c) and 1 μM valinomycin with 100 mM K^+ (panel d). **Panels e and f** show % increase in fluo4 fluorescence intensity with respect to mean fluorescence before the P4 stimulus (Δ fluorescence (%)) for the cells in videos 6 and 7 respectively. Grey shading shows period of exposure to 11 μM RU1968 (panel e) and 4.8 μM RU1968 (panel f).

Figure S3. Valinomycin sets V_m at E_K . Calculated E_K and the directly measured V_m (zero current clamp) are plotted against $\log [\text{K}^+]_o$. Black line shows relationship of calculated E_K to $[\text{K}^+]_o$, red dotted line shows mean V_m (\pm SEM) in the presence of 5.4 mM and 100 mM $[\text{K}^+]_o$.

Figure S4. RU1968 induces large, slow oscillation in some cells. Application of 3 μM P4 (arrow) induced a $[\text{Ca}^{2+}]_i$ transient but no oscillations were seen in these cells. However, upon application of 4.8 μM RU1968 a large, slow $[\text{Ca}^{2+}]_i$ oscillation was induced. Responses of 4 separate cells shown. $[\text{K}^+]_o = 5.4$ mM throughout.

Video file legends

- 692 **Video 1.** $[Ca^{2+}]_i$ oscillation. 151 frames recorded at 2.5 Hz. 10 Hz playback. $[Ca^{2+}]_i$ elevation in the
693 flagellum precedes that in the head. Original image size (height*width) = 37.6*10.45 μm
- 694 **Video 2.** 3 μM progesterone (P4)-induced $[Ca^{2+}]_i$ transient, same cell as video 1. 151 frames recorded
695 at 2.5 Hz. 10 Hz playback. P4 was applied at ≈ 2 s. $[Ca^{2+}]_i$ elevation in the flagellum precedes that in
696 the head. Original image size = 37.6*10.45 μm
- 697 **Video 3.** Cell stimulated with P4 (5 min) then co-exposed to 1 μM valinomycin (25-45 min). 840
698 frames recorded at 0.2 Hz. 20 Hz playback. Original image size = 13.2*22.4 μm
- 699 **Video 4.** Cell stimulated with P4 (5 min) then co-exposed to 1 μM valinomycin and 25 mM K^+ (25-45
700 min). 840 frames recorded at 0.2 Hz. 20 Hz playback. Original image size = 24.4*16.8 μm
- 701 **Video 5.** Cell stimulated with P4 (5 min) then co-exposed to 1 μM valinomycin and 100 mM K^+ (25-
702 45 min). 840 frames recorded at 0.2 Hz. 20 Hz playback. Original image size = 15.2*23.6 μm
- 703 **Video 6.** Cell stimulated with P4 (5 min) then co-exposed to 11 μM RU1968 (16-26 min). 481 frames
704 recorded at 0.2 Hz. 20 Hz playback. Original image size = 12.8*24 μm
- 705 **Video 7.** Cell stimulated with P4 (3.3 min) then co-exposed to 4.8 μM RU1968 (14-24 min). 433
706 frames recorded at 0.2 Hz. 20 Hz playback. Original image size = 16.8*16.8 μm
- 707

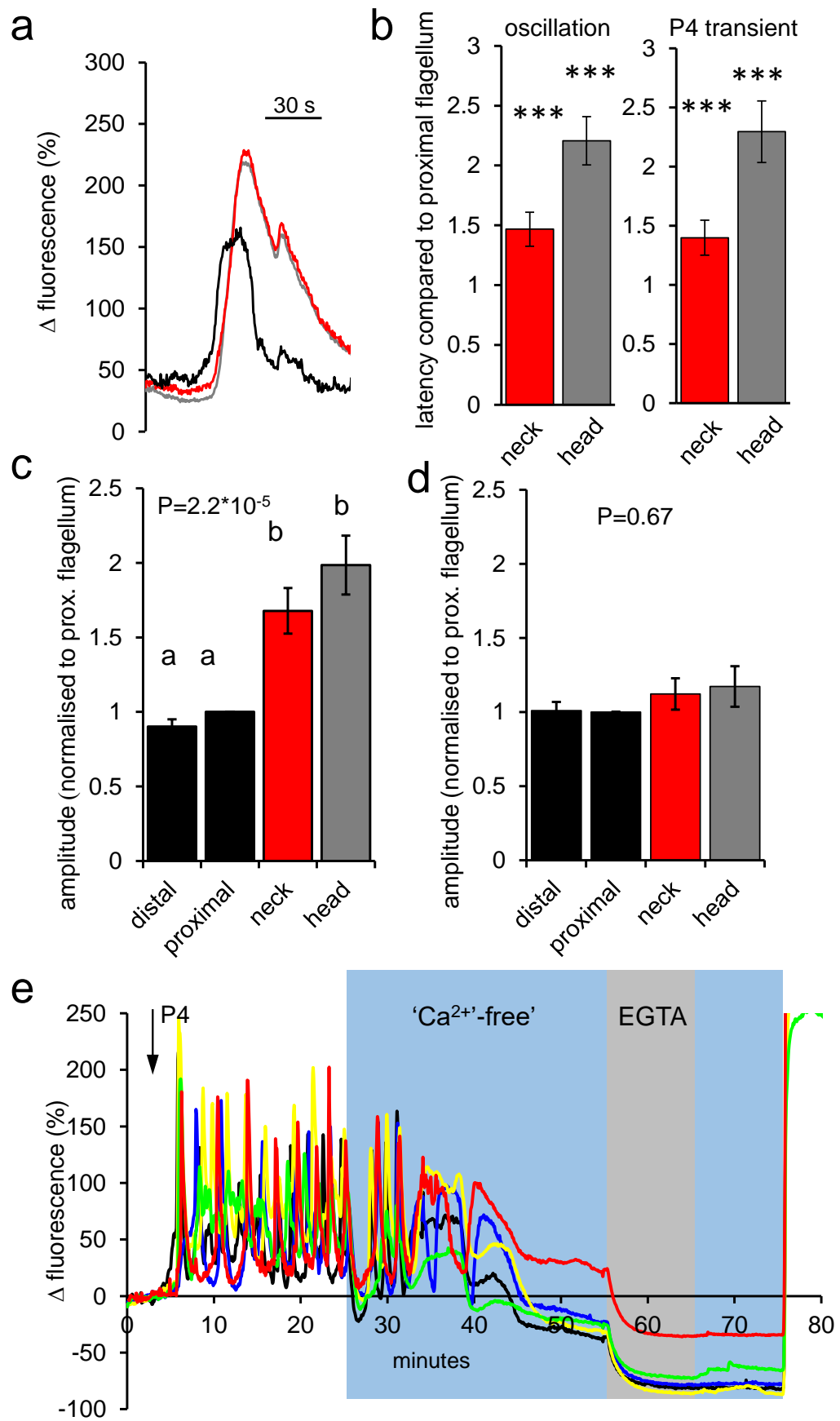


Fig 1

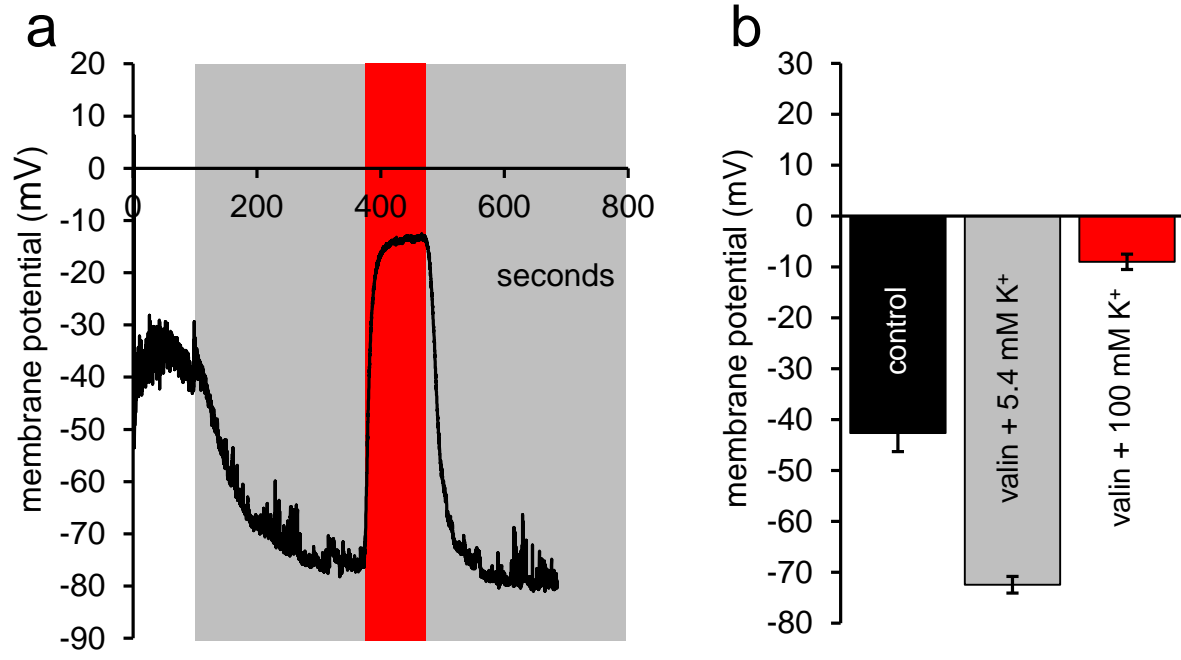


Fig 2

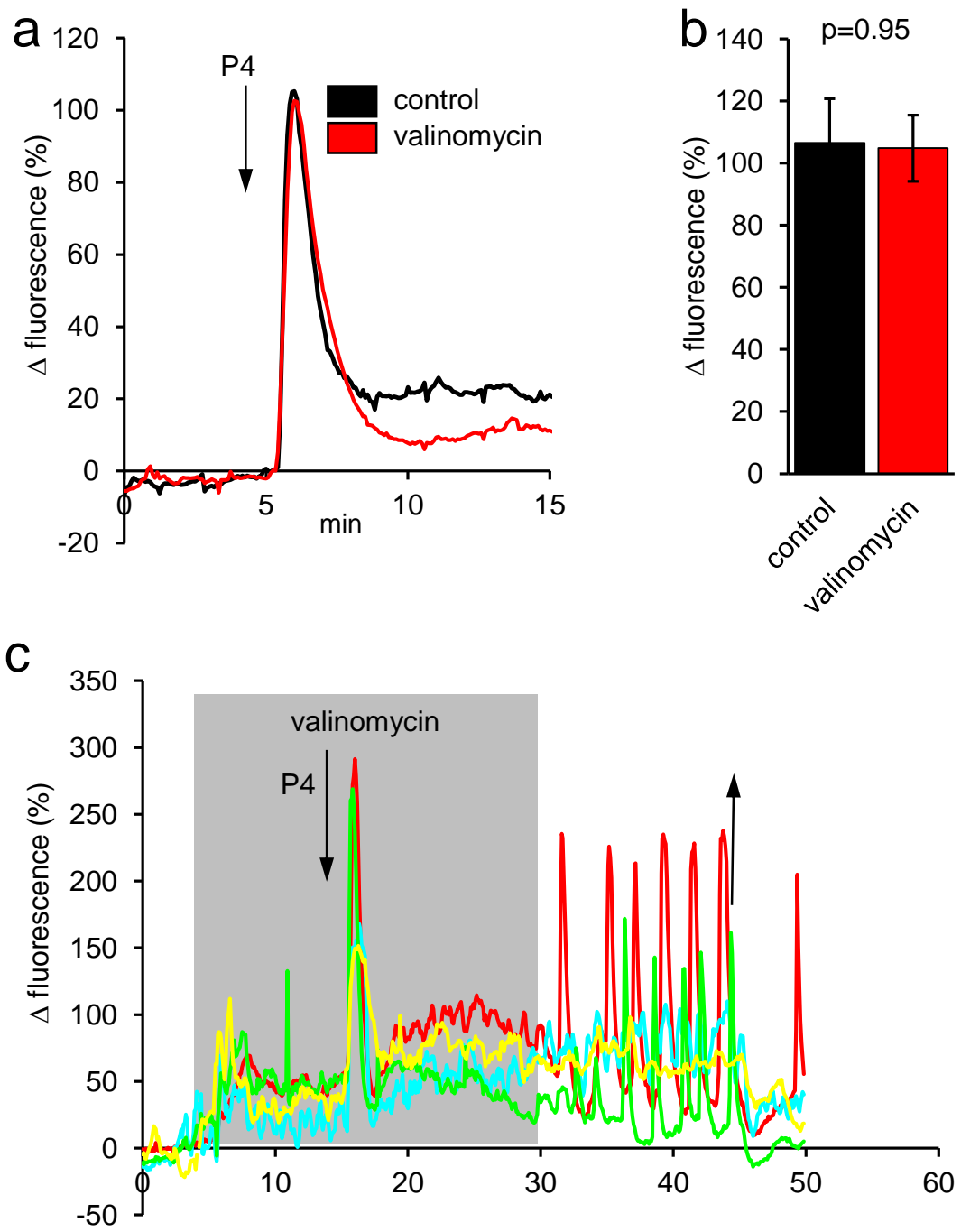


Fig 3

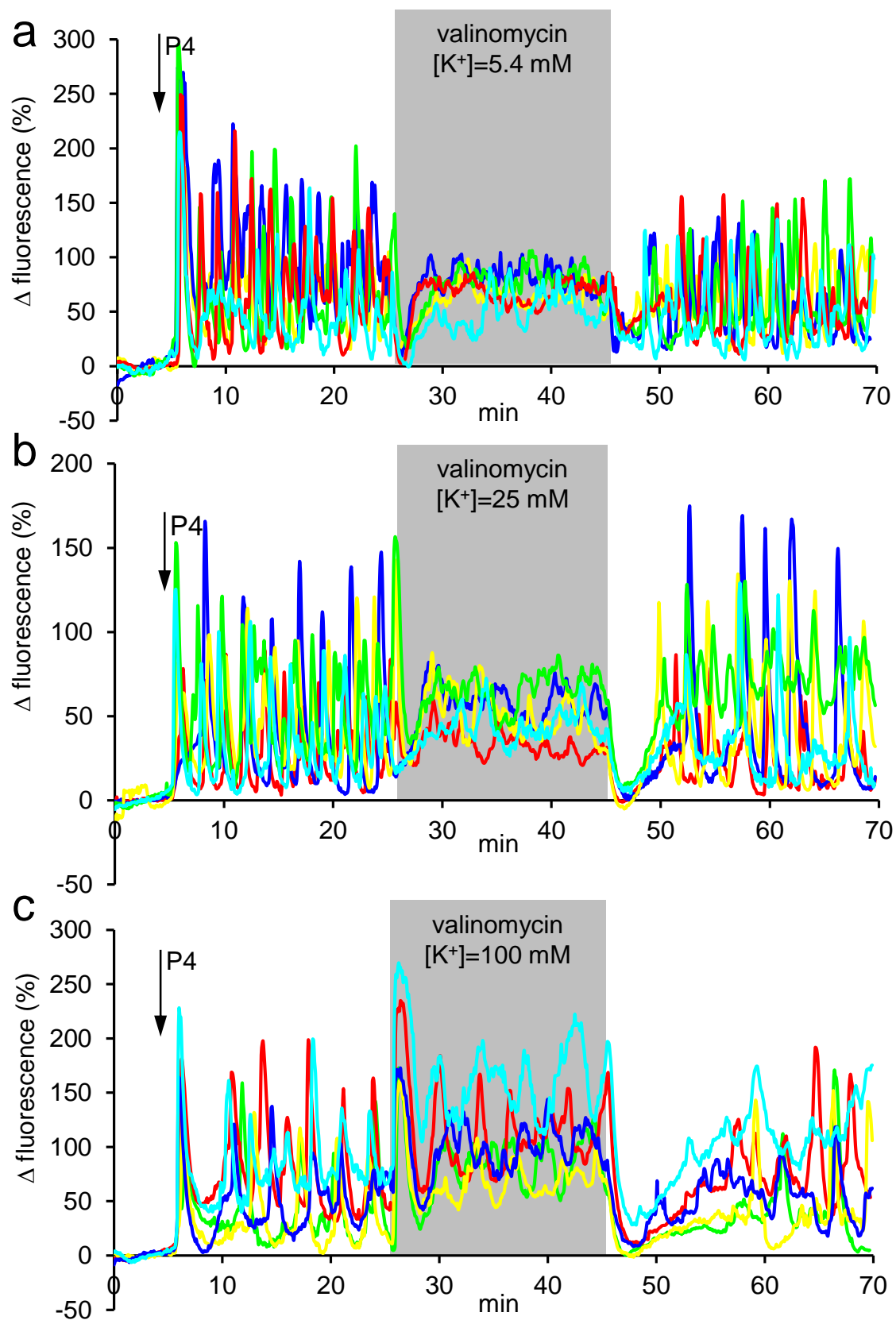


Fig 4

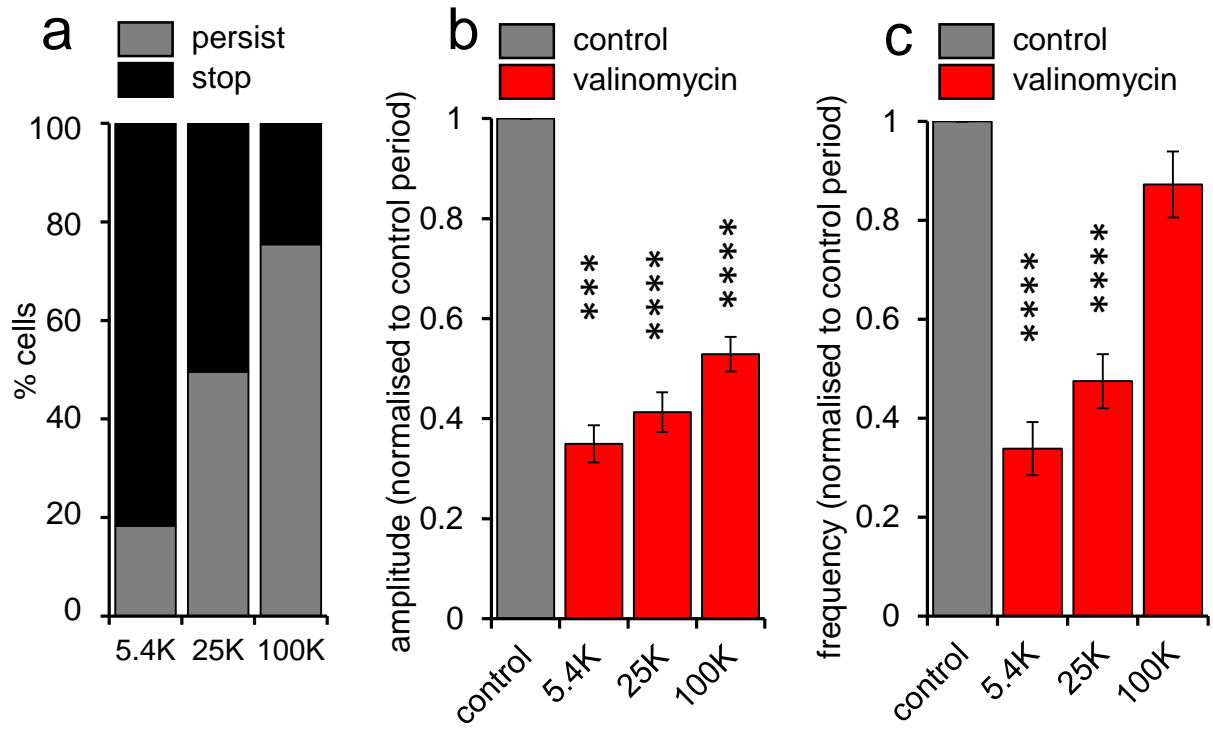
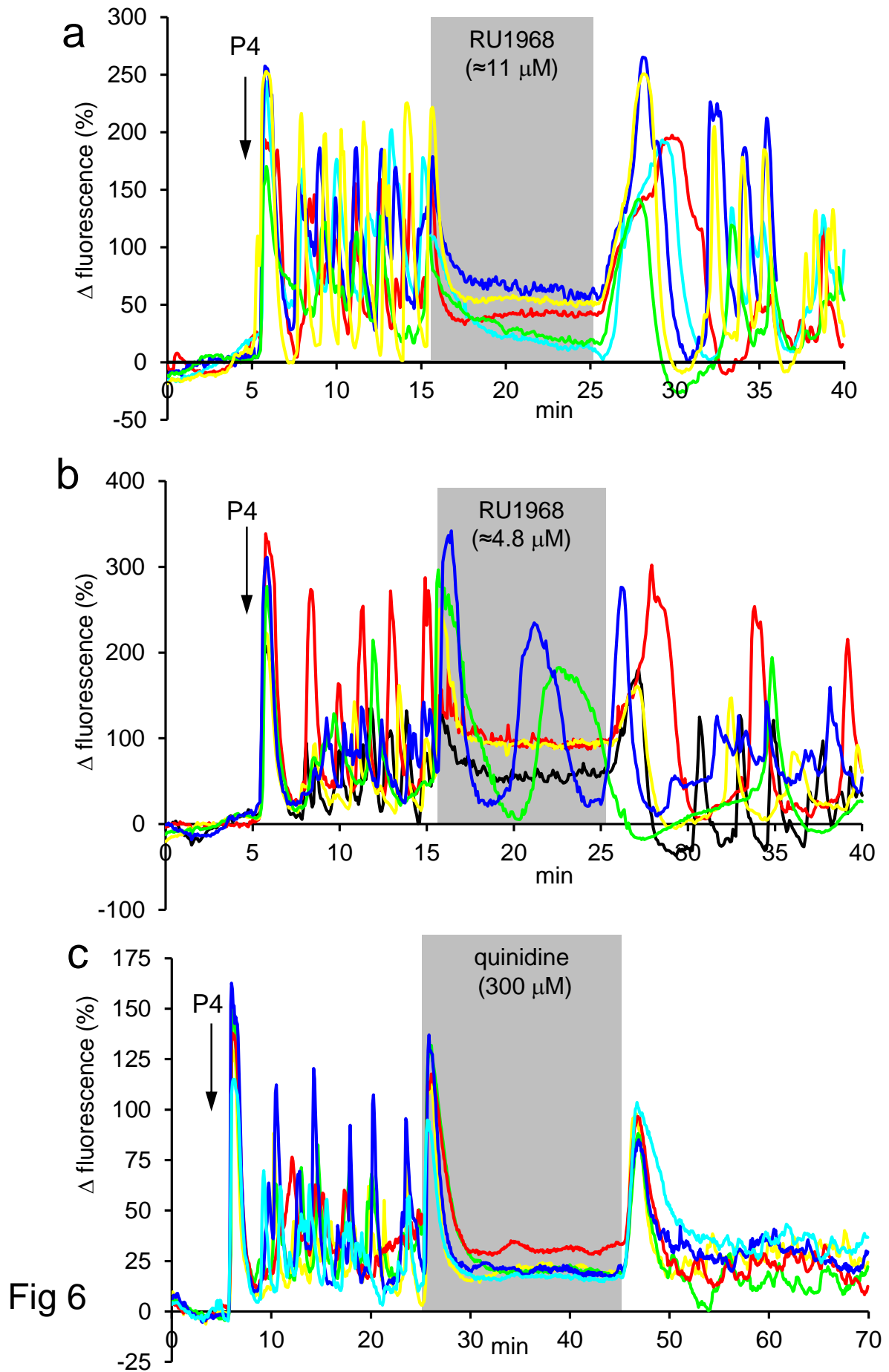


Fig 5



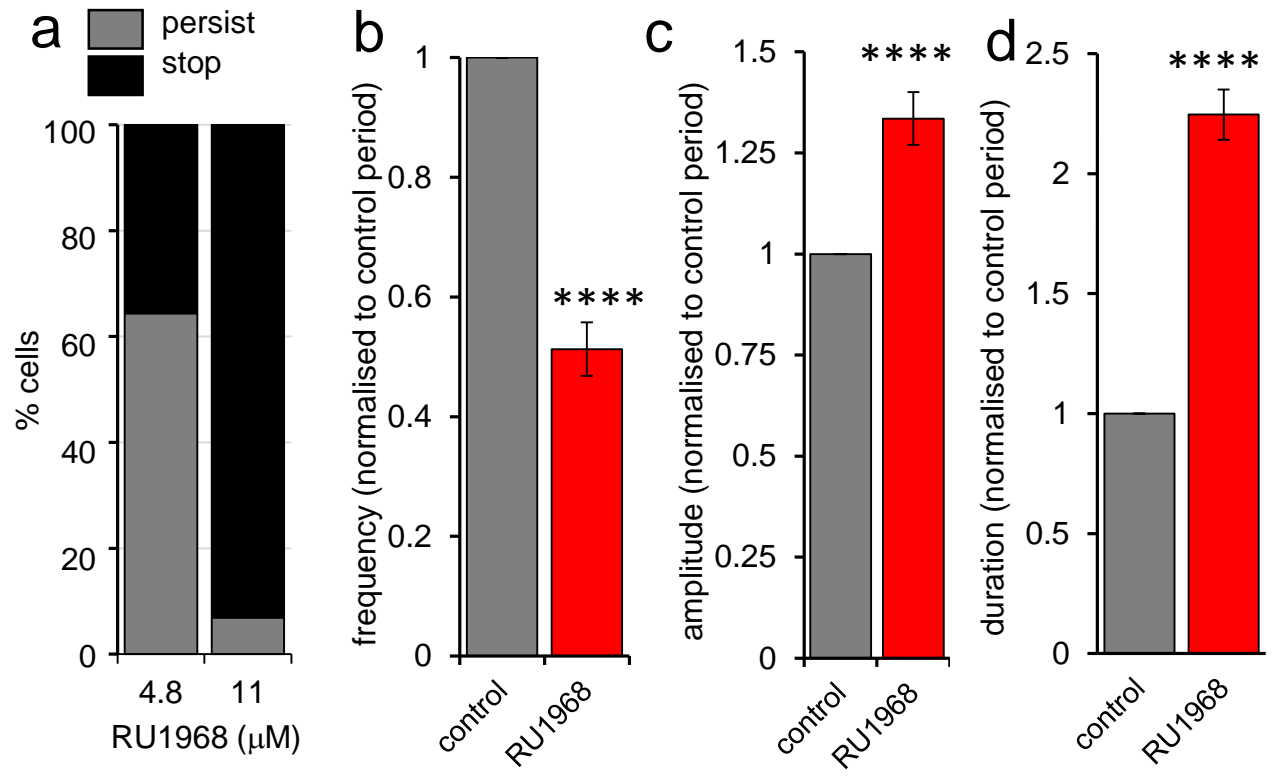


Fig 7

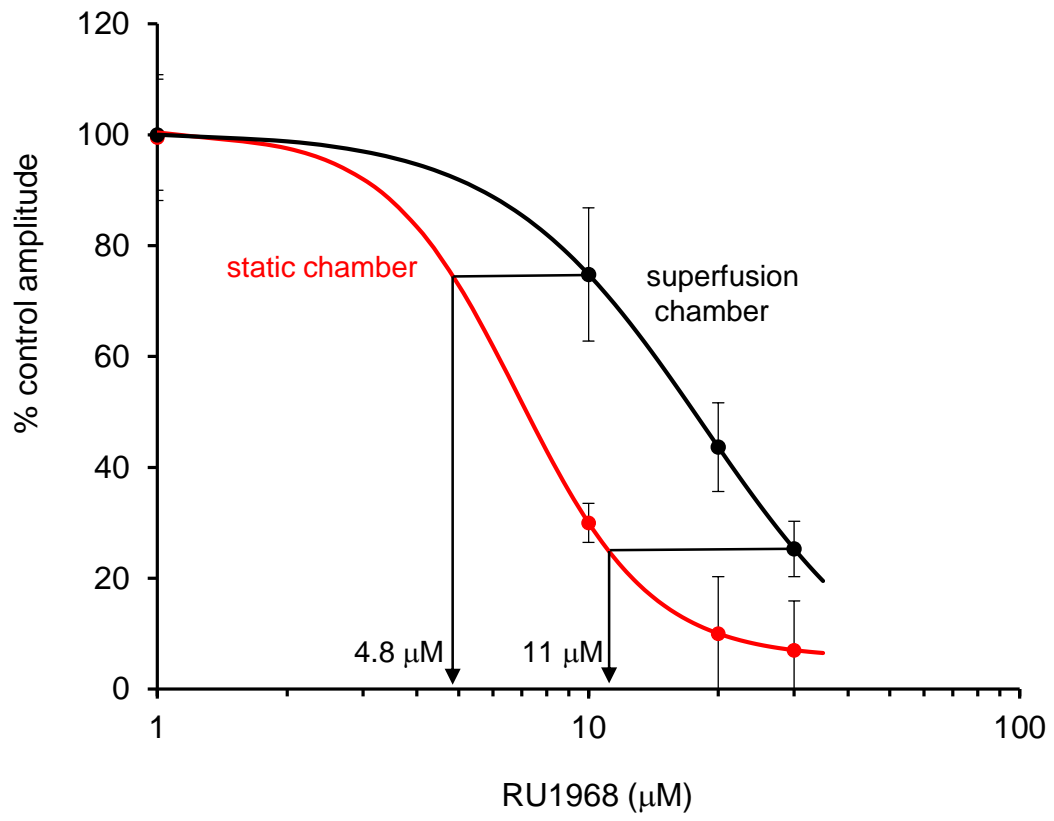


Fig S1

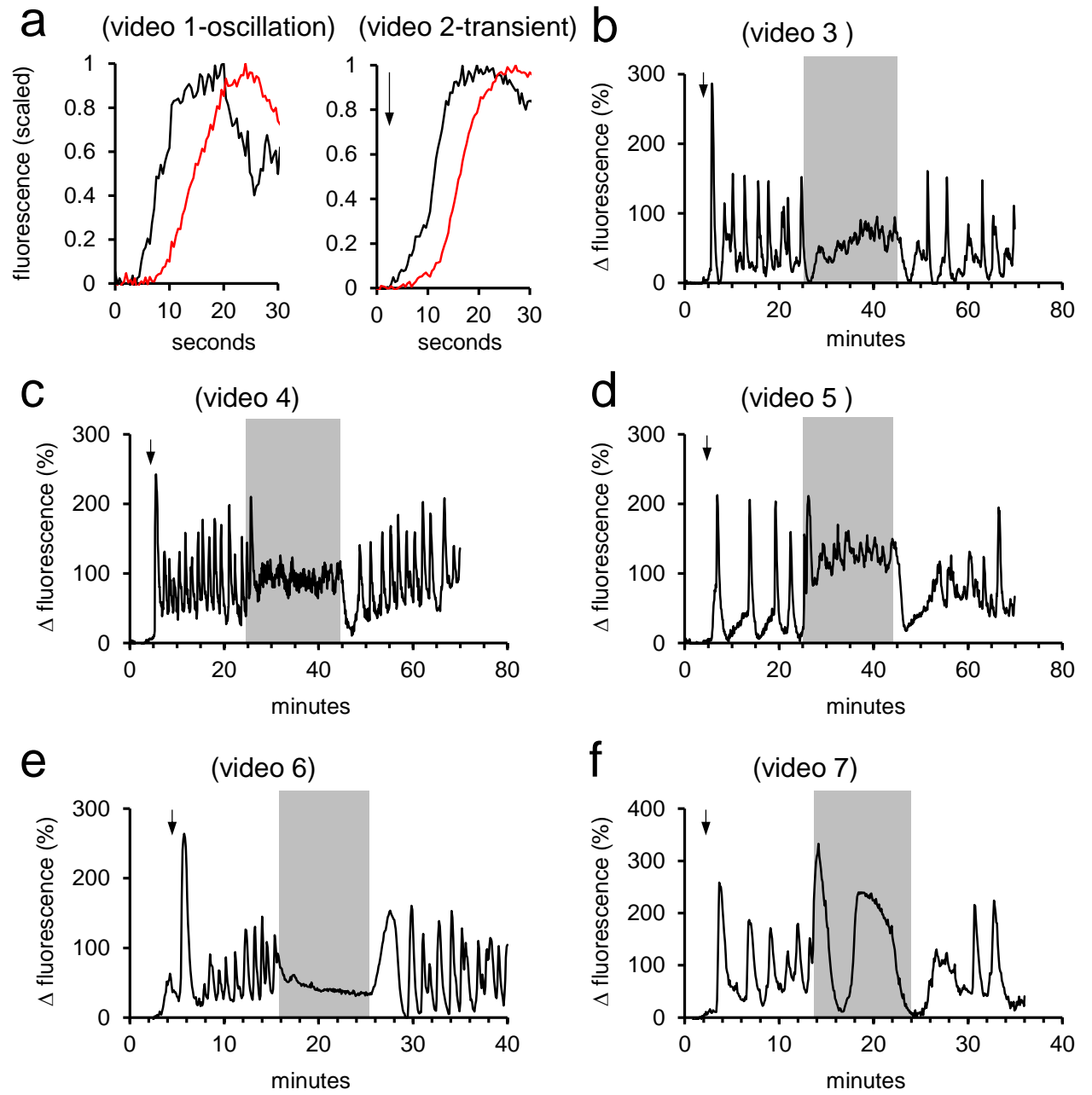


Fig S2

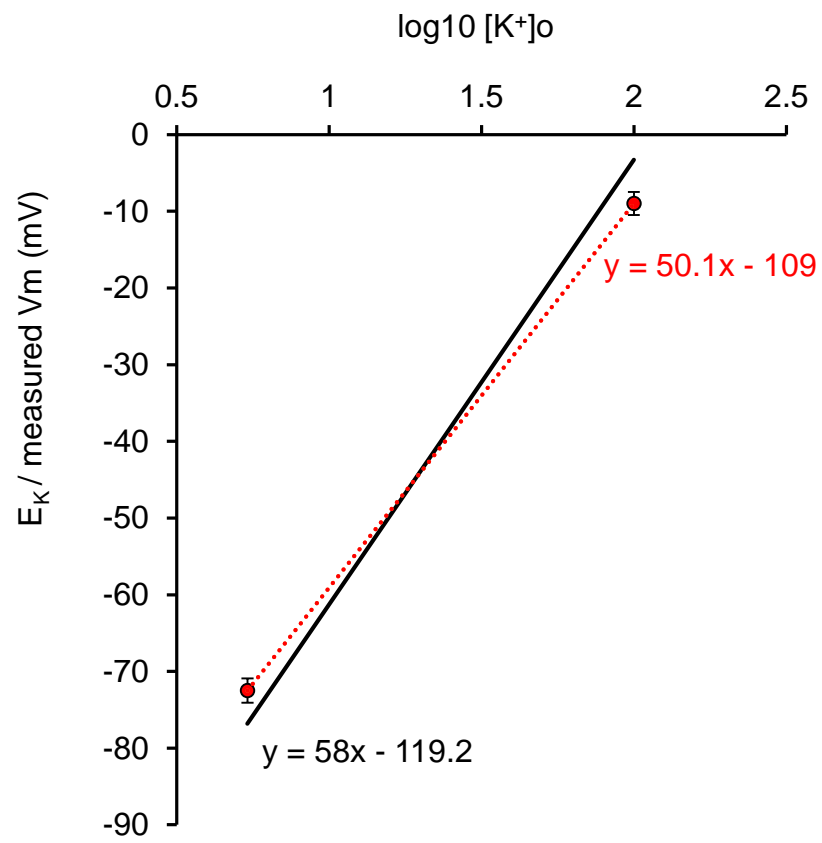


Fig S3

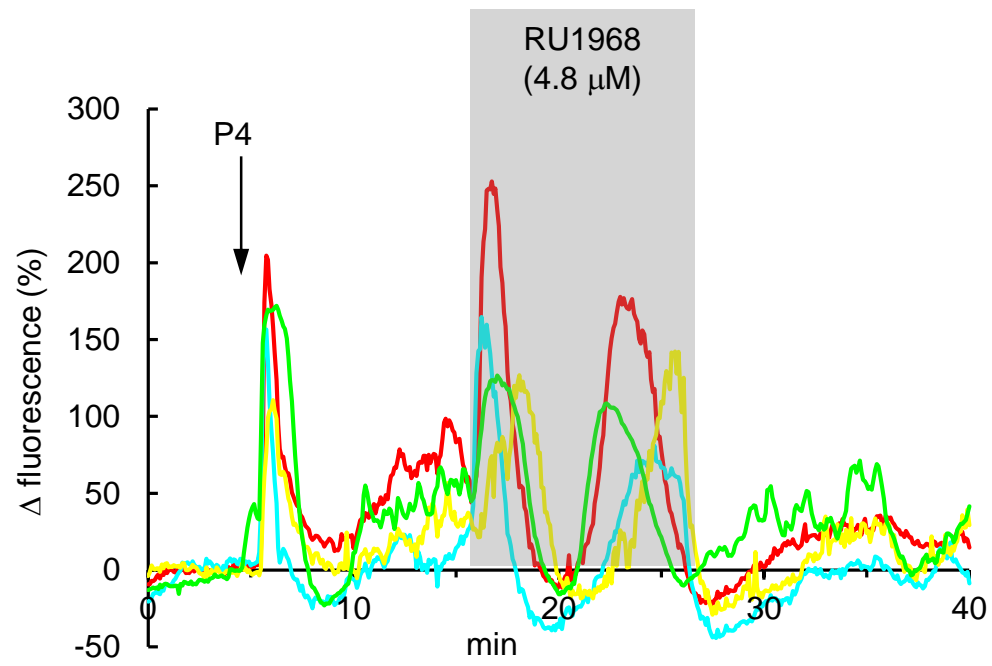


Fig S4